Science and Technology Facilities Council

Measurement of $e^+e^- \rightarrow \pi^+\pi^-\pi^0$ with ISR events at BaBar and its contribution to $(g-2)_\mu$

Fergus Wilson

Rutherford Appleton Laboratory

On behalf of the BaBar Collaboration

Brookhaven Forum 2021

Outline

- Recent BaBar results with multiple pions:
  - Preliminary measurement of $e^+e^- \to \pi^+\pi^-\pi^0$ cross-section
    - arXiv:2110.00520 ← Main result
  - Preliminary measurements of $e^+e^- \to \pi^+\pi^-4\pi^0$ cross-section
    - arXiv:2110.00823
  - First measurements of $e^+e^- \to 2(\pi^+\pi^-)3\pi^0$ cross-section
    - PRD 102, 092001 (2021)

- Contribution to $(g-2)_\mu$ from $e^+e^- \to \pi^+\pi^-\pi^0$
- Conclusion

BaBar at SLAC PEP-II: 1999 - 2008

- Asymmetric beam energies nominally colliding 3.1 GeV e^+ and 9.0 GeV e^- at (mostly) the Y(4S) resonance

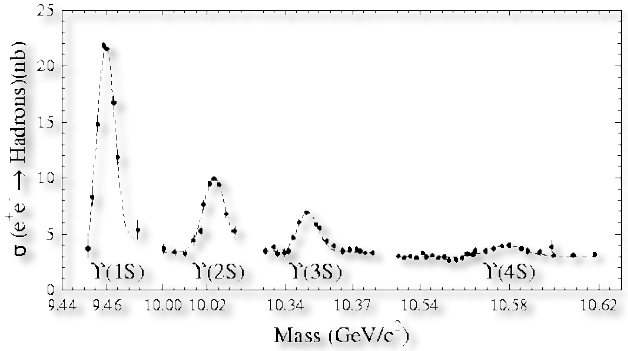

Advantages	Known initial state, low backgrounds, good tagging efficiency (30%), good neutral detection, quantum correlated B production, almost hermetic detectors
Disadvantages	Production x-section ~1 nb, limited B_s production, no B_c, no high mass baryons, limited Y(2,3,5S).

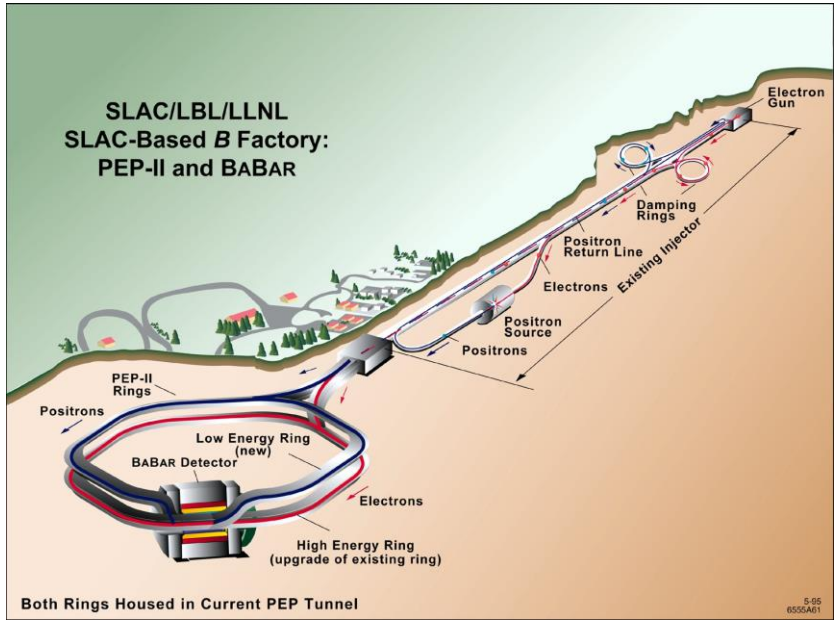

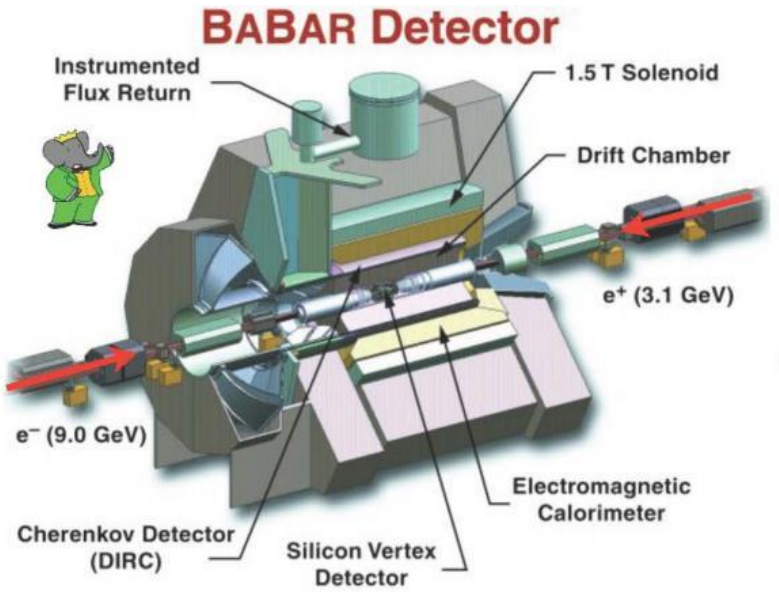

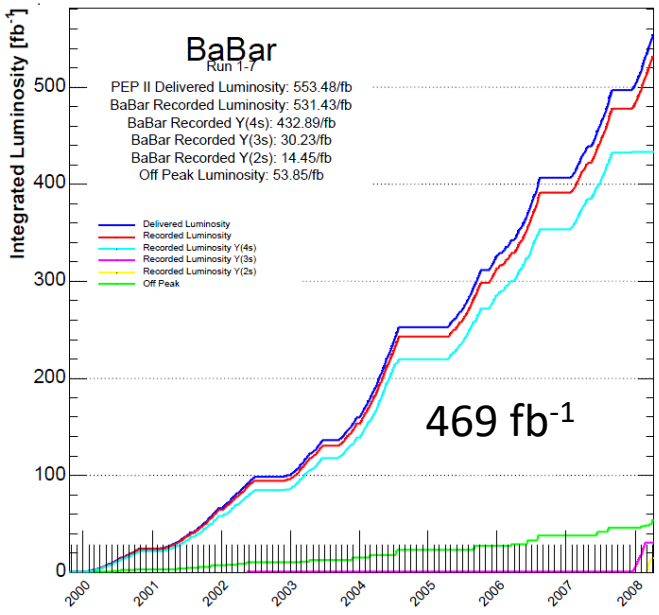

BaBar and ISR

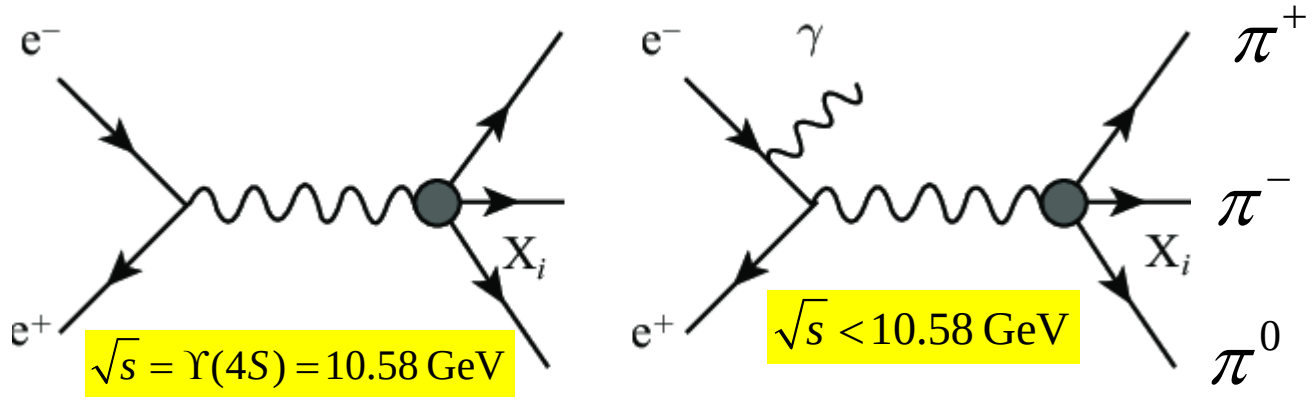

- Cross-sections can be measured down to threshold.
- Measure σ at all s simultaneously.
- About 10% of ISR γ's are produced in fiducial region of the BaBar detector ($30^o < \theta_\gamma < 150^o$).
- Tag event with presence of high energy ISR γ
- All hadrons in the detector.
- Fully reconstruct the final state.

$$\frac{d\sigma(s,x,\theta_\gamma)}{dx\, d\cos\theta_\gamma} = W(s,x,\theta_\gamma)\sigma_s(s(1-x))$$

$$W(s,x,\theta_\gamma) = \frac{\alpha}{2\pi}\left(\frac{2-2x+x^2}{\sin^2\theta_\gamma} - \frac{x^2}{2}\right)$$

$$x = 2E_\gamma / \sqrt{s}$$

$e^+e^- \longrightarrow \pi^+\pi^-\pi^0$ contribution to $a_\mu = (g-2)_\mu/2$

- SM prediction: $a_\mu^{SM} = \frac{(g-2)_\mu}{2} = a_\mu^{QED} + a_\mu^{EW} + a_\mu^{Had}$
- Leading order hadronic contribution:

$$a_\mu^{Had,LO} = \frac{\alpha^2}{3\pi^2}\int_{m_\pi^2}^{\infty}\frac{K(s)}{s}\frac{\sigma_0(e^+e^- \to hadrons)(s)}{4\pi\alpha^2/3s}$$

$$K(s) = \frac{x^2}{2}(2-x^2) + \frac{(1+x^2)(1+x)^2}{x^2}\left(\log(1+x) - x + \frac{x^2}{2}\right) + \frac{1+x}{1-x}x^2\log x$$

$$x = \frac{1-\beta}{1+\beta},\ \beta = \sqrt{1-4m_\mu^2/s}$$

- (for details, see [1] for example)
- $e^+e^- \to \pi^+\pi^-$ contributes ~73% to $a_\mu^{Had,LO}$
- $e^+e^- \to \pi^+\pi^-\pi^0$ next largest at ~7% [2]

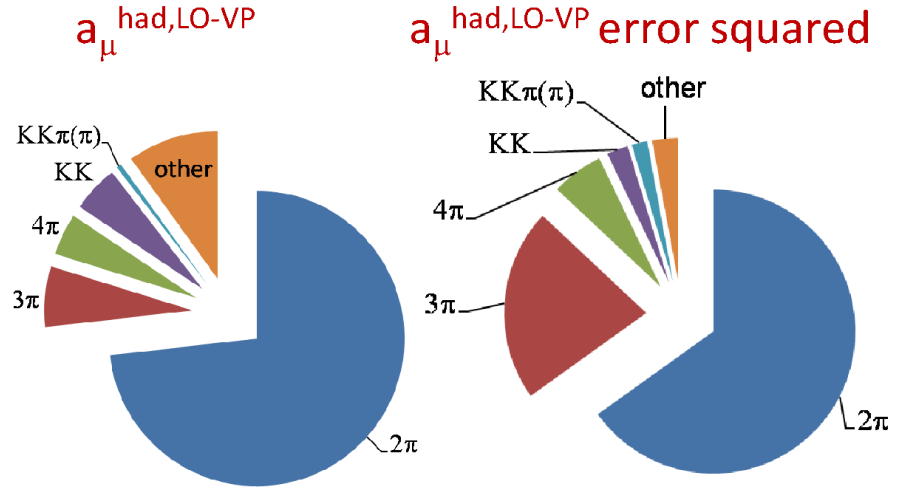

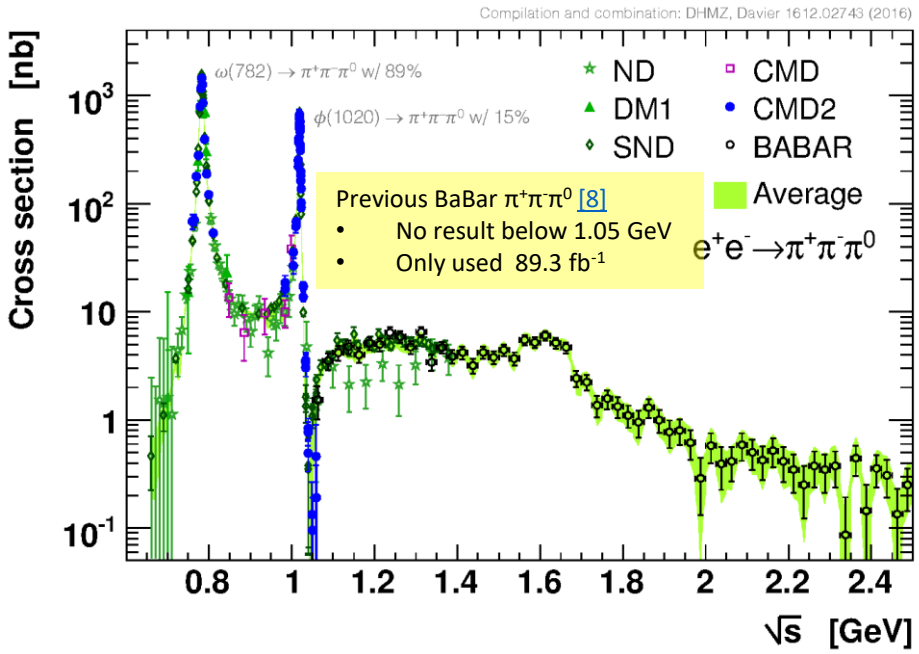

$e^+e^- \to \pi^+\pi^-\pi^0\gamma_{ISR}$ selection

- Two good oppositely charged tracks + 3 or more γ's
  - $E(\gamma_{ISR}) > 3$ GeV and $0.10 < M_{\pi^0} < 0.17$ GeV
- Select events using a kinematic fit (cut on fit quality, χ^2)
- Reduce backgrounds through e.g.
  - Particle Identification (K/π), energy of π^0, mass of $\pi\pi$ and $\pi^{\pm}\gamma_{ISR}$ pairs, fit to alternative decay hypotheses (e.g. $e^+e^- \to \pi^+\pi^-\pi^0\pi^0\gamma$), …
- Remaining ISR and $q\bar{q}$ background subtraction:
  - $M_{3\pi} < 1.1$ GeV: use simulation, reweighted using data. Background fraction ~2%.
  - $M_{3\pi} > 1.1$ GeV: many ISR processes not simulated, so number of background events extrapolated using data from $20 < \chi^2 < 40$ region. Background fraction 10%-15%.

$e^+e^- \to \pi^+\pi^-\pi^0$ mass spectrum

arXiv:2110.00520

Fit with Vector Dominance Model (VDM) to $M_{3\pi}$ distribution with detector resolution effects unfolded:

Spectrum varies by 4 orders of magnitude and has two narrow peaks (ω,ϕ)

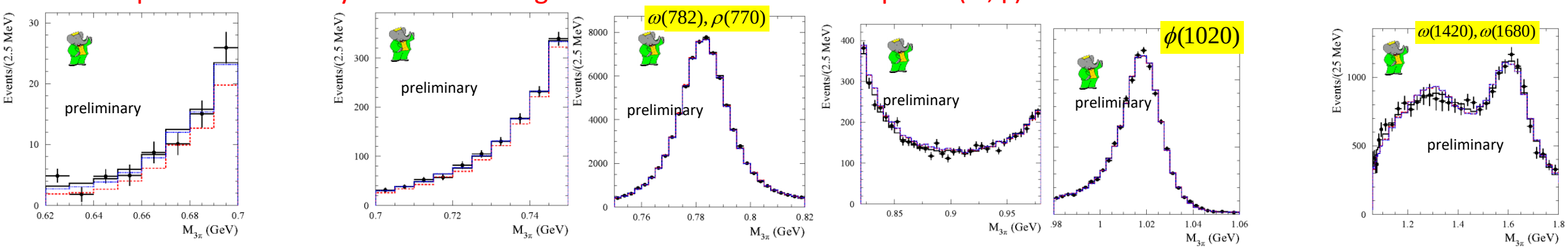

Colored lines represent different fit models. Best fit (solid/black) includes presence of $\rho \to \pi\pi\pi$

Fit includes: $\omega(782)+\omega(1420)+\omega(1680)+\phi(1020)+\rho(770) \to 3\pi$

	BaBar	Comparison
$\Gamma(\omega \to e^+e^-)\beta(\omega \to \pi^+\pi^-\pi^0)$	$(0.5698 \pm 0.0031 \pm 0.0082)$ keV	$WA: (0.557 \pm 0.011)$ keV
$\Gamma(\phi \to e^+e^-)\beta(\phi \to \pi^+\pi^-\pi^0)$	$(0.1841 \pm 0.0021 \pm 0.0080)$ keV	$WA: (0.1925 \pm 0.0043)$ keV
$\beta(\rho \to \pi^+\pi^-\pi^0)$	$(0.88 \pm 0.23 \pm 0.30)$ x 10^{-4}	$SND: (1.01^{+0.54}_{-0.34} \pm 0.34)\text{x}10^{-4}$
$(\phi_\rho - \phi_\omega)$	$-(99 \pm 9 \pm 15)^o$	$SND: -(135^{+17}_{-13} \pm 9)^0$

$e^+e^- \longrightarrow \pi^+\pi^-\pi^0$ cross-section: comparison with SND/CMD-2

Differences between experiments have been a source of systematic uncertainty on $(g\text{-}2)_\mu$ for some time

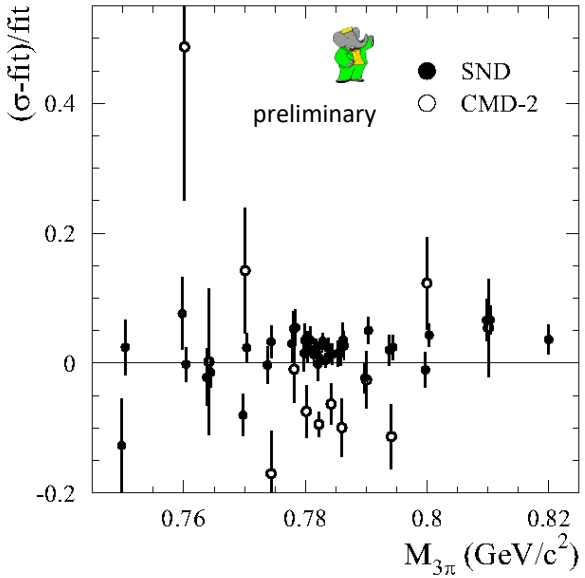

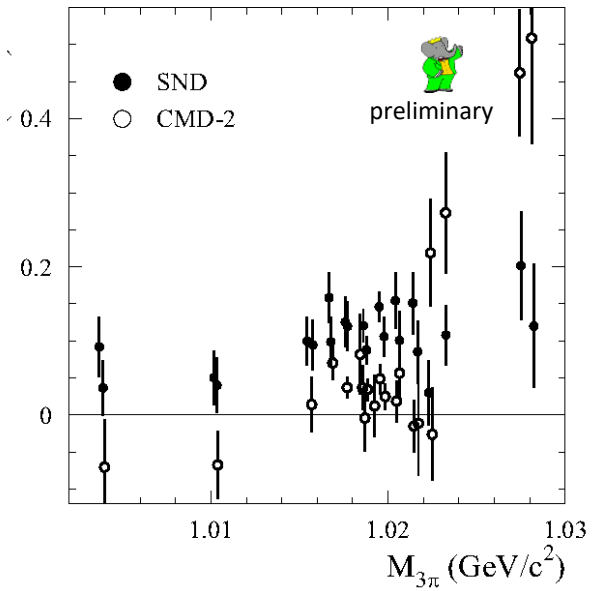

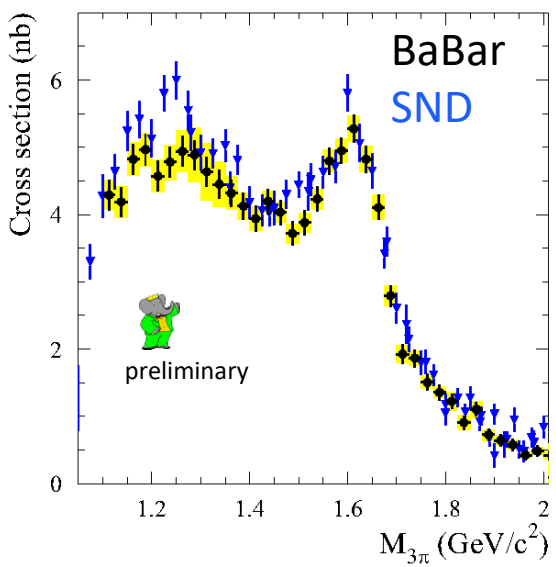

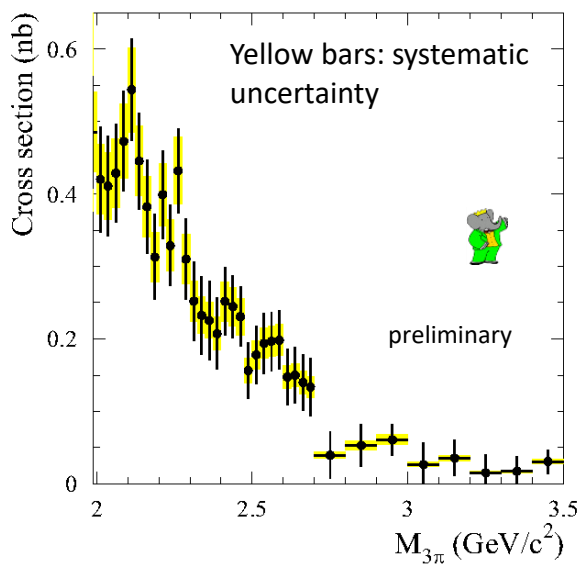

Δ(SND-BaBar) = 2%
Δ(CMD-2-BaBar) = 7%

Δ(SND-BaBar) = 11%
Δ(CMD-2-BaBar) = 3%

Generally good agreement but differences between SND and BaBar near 1.25 and 1.5 GeV

SND results: [3], [4], [7] ; CMD-2 results [5], [6]

$e^+e^- \longrightarrow \pi^+\pi^-4\pi^0$

arXiv:2110.00823

- Similar selection technique to $e^+e^- \longrightarrow \pi^+\pi^-\pi^0$
- Same integrated luminosity (469 fb^{-1})
- Many branching fractions and cross-sections measured for the first time.

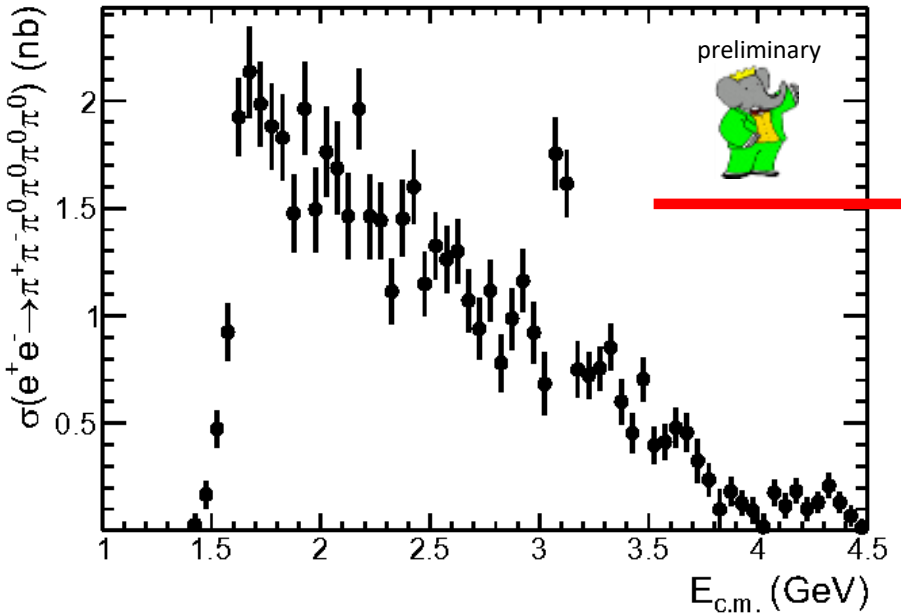

Statistical uncertainty 12%-15%

TABLE I: Summary of the $e^+e^- \to \pi^+\pi^-\pi^0\pi^0\pi^0\pi^0$ cross section measurement. The uncertainties are statistical only.

$E_{c.m.}$ (GeV)	σ (nb)	$E_{c.m.}$ (GeV)	σ (nb)	$E_{c.m.}$ (GeV)	σ (nb)	$E_{c.m.}$ (GeV)	σ (nb)	$E_{c.m.}$ (GeV)	σ (nb)
1.425	0.03 ± 0.05	2.075	1.69 ± 0.21	2.725	0.94 ± 0.14	3.375	0.60 ± 0.10	4.025	0.02 ± 0.06
1.475	0.17 ± 0.06	2.125	1.46 ± 0.20	2.775	1.12 ± 0.14	3.425	0.45 ± 0.09	4.075	0.18 ± 0.06
1.525	0.47 ± 0.08	2.175	1.96 ± 0.19	2.825	0.78 ± 0.13	3.475	0.71 ± 0.10	4.125	0.11 ± 0.06
1.575	0.92 ± 0.13	2.225	1.46 ± 0.19	2.875	0.99 ± 0.14	3.525	0.40 ± 0.08	4.175	0.18 ± 0.06
1.625	1.92 ± 0.18	2.275	1.44 ± 0.18	2.925	1.16 ± 0.14	3.575	0.41 ± 0.08	4.225	0.10 ± 0.05
1.675	2.13 ± 0.21	2.325	1.11 ± 0.15	2.975	0.92 ± 0.14	3.625	0.48 ± 0.09	4.275	0.13 ± 0.05
1.725	1.99 ± 0.20	2.375	1.45 ± 0.18	3.025	0.68 ± 0.15	3.675	0.46 ± 0.09	4.325	0.21 ± 0.06
1.775	1.88 ± 0.20	2.425	1.60 ± 0.17	3.075	1.75 ± 0.17	3.725	0.32 ± 0.10	4.375	0.13 ± 0.05
1.825	1.83 ± 0.20	2.475	1.15 ± 0.15	3.125	1.61 ± 0.16	3.775	0.24 ± 0.08	4.425	0.07 ± 0.05
1.875	1.48 ± 0.18	2.525	1.33 ± 0.16	3.175	0.75 ± 0.13	3.825	0.10 ± 0.09	4.475	0.01 ± 0.04
1.925	1.96 ± 0.21	2.575	1.26 ± 0.16	3.225	0.72 ± 0.10	3.875	0.18 ± 0.07		
1.975	1.49 ± 0.20	2.625	1.30 ± 0.15	3.275	0.75 ± 0.10	3.925	0.13 ± 0.06		
2.025	1.76 ± 0.21	2.675	1.07 ± 0.14	3.325	0.85 ± 0.11	3.975	0.10 ± 0.06		

- Preprint also includes cross-sections for $e^+e^- \longrightarrow \omega 3\pi^0$, $\eta\pi^+\pi^-\pi^0$ and $\omega\eta$

$e^+e^- \to 2(\pi^+\pi^-)3\pi^0$ and $e^+e^- \to 2(\pi^+\pi^-)2\pi^0\eta$ PRD 102, 092001 (2021)

- Similar selection technique again. Same integrated luminosity (469 fb^{-1}). Many branching fractions and cross-sections measured for the first time.

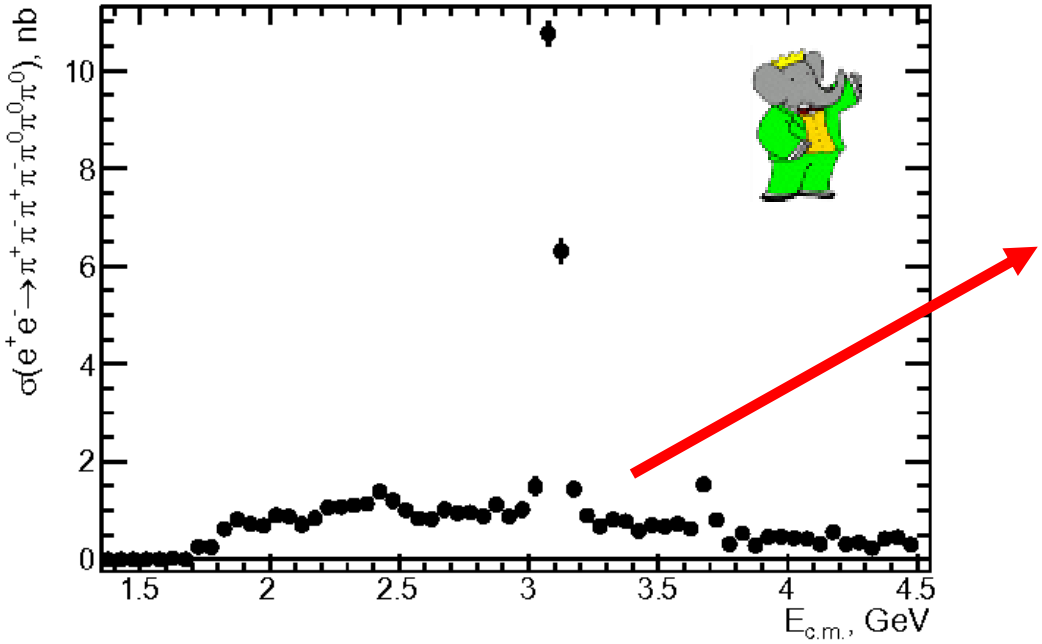

TABLE I: Summary of the $e^+e^- \to 2(\pi^+\pi^-)3\pi^0$ cross section measurement. The uncertainties are statistical only.

$E_{c.m.}$, GeV	σ, nb	$E_{c.m.}$, GeV	σ, nb	$E_{c.m.}$, GeV	σ, nb	$E_{c.m.}$, GeV	σ, nb	$E_{c.m.}$, GeV	σ, nb
1.575	0.00 ± 0.01	2.175	0.84 ± 0.15	2.775	0.96 ± 0.14	3.375	0.78 ± 0.12	3.975	0.46 ± 0.09
1.625	0.02 ± 0.01	2.225	1.06 ± 0.11	2.825	0.88 ± 0.13	3.425	0.59 ± 0.09	4.025	0.44 ± 0.09
1.675	0.00 ± 0.02	2.275	1.07 ± 0.14	2.875	1.12 ± 0.13	3.475	0.70 ± 0.11	4.075	0.42 ± 0.09
1.725	0.26 ± 0.06	2.325	1.11 ± 0.12	2.925	0.88 ± 0.13	3.525	0.67 ± 0.10	4.125	0.32 ± 0.07
1.775	0.25 ± 0.07	2.375	1.14 ± 0.14	2.975	1.02 ± 0.17	3.575	0.73 ± 0.12	4.175	0.56 ± 0.08
1.825	0.62 ± 0.09	2.425	1.39 ± 0.16	3.025	1.49 ± 0.20	3.625	0.63 ± 0.11	4.225	0.31 ± 0.08
1.875	0.82 ± 0.14	2.475	1.21 ± 0.16	3.075	10.76 ± 0.26	3.675	1.53 ± 0.15	4.275	0.35 ± 0.06
1.925	0.73 ± 0.09	2.525	1.01 ± 0.16	3.125	6.30 ± 0.26	3.725	0.81 ± 0.13	4.325	0.23 ± 0.07
1.975	0.69 ± 0.10	2.575	0.84 ± 0.14	3.175	1.44 ± 0.15	3.775	0.31 ± 0.11	4.375	0.42 ± 0.06
2.025	0.90 ± 0.15	2.625	0.82 ± 0.11	3.225	0.90 ± 0.11	3.825	0.53 ± 0.10	4.425	0.45 ± 0.07
2.075	0.88 ± 0.14	2.675	1.02 ± 0.15	3.275	0.67 ± 0.12	3.875	0.29 ± 0.09	4.475	0.30 ± 0.07
2.125	0.70 ± 0.16	2.725	0.95 ± 0.15	3.325	0.82 ±0.12	3.925	0.46 ± 0.09		

- Paper also includes cross-sections for $e^+e^- \to \omega\,\pi^+\pi^-\pi^0\pi^0$, $\eta\pi^+\pi^-\pi^0\pi^0$ and $\eta 2(\pi^+\pi^-)$

$e^+e^- \longrightarrow \pi^+\pi^-\pi^0$ contribution to $(g\text{-}2)_\mu$

$M_{3\pi}$ GeV/c^2	$a_\mu^{3\pi}\left[10^{-10}\right]$	Ref.
$0.62-1.10$	$42.91\pm0.14\pm0.55\pm0.09$	
$1.10-2.00$	$2.95\pm0.03\pm0.16$	
<2.00	$45.86\pm0.14\pm0.58$	
<1.80	$46.21\pm0.40\pm1.40$	Eur. Phys. J. C 80, 241(2020)
<1.97	46.74 ± 0.94	Phys. Rev. D 101, 014029 (2020)
<2.00	44.32 ± 1.48	Springer Tracts Mod. Phys. 274, 1 (2017)

Differences in 3π mass scales between experiments.

Estimated from differences in BaBar/SND/CMD-2 data

Effect	Uncertainty (%)
Luminosity	0.4
Radiative correction	0.5
Detection efficiency	1.1
MC statistics	0.15
Background subtraction	0.073
Gaussian smearing	0.0007
Lorentzian smearing	0.003
Unfolding procedure	0.045
Total	1.3

Conclusion

- We have presented a number of recent measurements of the process $e^+e^- \rightarrow$ hadrons + γ_{ISR} .
- Cross-sections for $e^+e^- \rightarrow 2(\pi^+\pi^-)3\pi^0$, $2(\pi^+\pi^-)2\pi^0\,\eta$, $\pi^+\pi^-4\pi^0$, and $\pi^+\pi^-3\pi^0\,\eta$ have been measured for the first time, using the ISR method with 469 fb^{-1} of data collected by BaBar at PEP-II at SLAC [arXiv:2110.00823, PRD 102, 092001 (2021)].
- Cross-sections can be measured from threshold up to ~4.5 GeV.
- The cross-section for $e^+e^- \rightarrow \pi^+\pi^-\pi^0$ has been measured in the center of mass range 0.62 – 3.5 GeV. [arXiv:2110.00520].
- The leading order hadronic contribution of $e^+e^- \rightarrow \pi^+\pi^-\pi^0$ to the muon anomalous magnetic moment has been calculated as $(45.86 \pm 0.14 \pm 0.58) \times 10^{-10}$ for $M_{3\pi} < 2.0$ GeV:
  - The contribution is in agreement with existing calculations but a factor of 2 more precise.